

Research Article



Subsurface Structural Characterization as Deduced from High-Resolution Aeromagnetic Data over The Confluence Zones in Central, Nigeria

Emmanuel Agada Anthony ¹, Othniel Kamfani Likkason ¹, Abubakar Sadiq Maigari ², Sani Ali ¹, Adamu Abubakar ³

¹Department of Physics, Abubakar Tafawa Balewa University, Bauchi, Nigeria

²Department of Applied Geology, Abubakar Tafawa Balewa University, Bauchi, Nigeria

³Department of Applied Geophysics, Federal University Birnin Kebbi, Nigeria

Correspondence: eaanthony13@gmail.com

Received: 14 March 2023 / Accepted: 15 May 2023 / Published: 21 May 2023

Abstract: This study aimed to delineate the intrusion body that controls the structural setting and formation around the river Niger-Benue confluence zone with particular attention to its solid mineral potentials, this is achieved in mapping subsurface structural features through the analysis of recent high-resolution aeromagnetic (HRAM) datasets with the purpose of examining their effects on geological structures that characterize the confluence zones from the study area. To obtain the necessary reduction in geomagnetic variation, measurements of regional gradients and time variation were used. After applying the reduction to the magnetic equator (RTE) to the corrected magnetic data that was obtained from the Nigerian Geological Survey Agency, NGSA, it was possible to determine the regional expansions of subsurface structural units for both qualitative and quantitative interpretations. In addition, the edge detection method is used to depict the structures and buried subsurface anomalies. Different handling processes were applied to the (HRAM) data, such as local wavenumber (SPI), power spectrum analysis, and Euler and Werner deconvolution analysis. The RTE magnetic anomaly caused by local structures and anomalous body delineated six sub-basins with low amplitude response, which agrees with the total gradient anomaly (analytic signal) and tilt of angle derivative that clearly outlined and characterize edges of lithostratigraphic of Niger-Benue river confluence zones. The sub-basin delineated are the southern Bida basin and northern Anambra basin. The source parameter imagings as well as the Euler and Werner deconvolution were used to delineate major subsurface structures and determine their source depth. Results showed that the area was affected by different lineament trending NE-SW, E-W, and S-E trends. Directional analysis indicates that the dominant trend agrees with the regional fault orientations. The estimated depth to the top of the lineaments on average varies from 0.3 km to 4.6 km and it is relatively deeper in the basins compared to the surrounding areas giving clues to the amount of sediment infill. A 2D forward model showed a sedimentary thickness ranging from 1 to 7 km, and this estimated depth is consistent with the average of 3.5 km proposed by previous researchers.

Keywords: Aeromagnetic data; Depth to basement; Edge detection techniques; Niger-Benue river confluence zone; Subsurface structures

INTRODUCTION

The Niger-Benue river confluence zones in North-central Nigeria have a total sediment thickness of about 5.5 km and present an economically viable solid mineral potential. It has a high degree of lithologic variability in both the literal and vertical extension. It is derived from a range of paleoenvironmental contexts dating from the Campanian to the Recent (Akaegbobi, 2005). The search for structural control commercial solid mineral potential in the area of study has been ongoing by mining cadaster, Initial efforts by oil companies, and research groups were unsatisfactory, leading to the neglect of these confluence zones in favor of the Niger Delta Basin. With increasing global energy demand and the advent of improved exploration, technology efforts are yielding positive results in the study area. With this situation, it has become necessary to delineate the intrusion body that controls the structural setting and formation around the river Niger-Benue confluence zone with particular attention to its solid mineral potentials, hence this study.

High-resolution aeromagnetic data are useful for the geologic and hydrologic mapping at a variety of scales, and also for environmental investigations. This paper discusses some of the guidelines

used in analyzing high-resolution aeromagnetic surveys and illustrates some of the techniques and software tools used for reducing, processing and interpreting such aeromagnetic data for structural and tectonic features. Reduction-to-the-magnetic equator (RTE) is a filtering technique used to align the peaks and gradients of the magnetic anomalies directly over their sources. This is a basic method for improving realistic estimations of source locations. Power spectrum transformation and source parameter imaging (SPI) filtering are techniques used to separate magnetic anomalies produced at different source depths. Anomalies caused by near-surface sources, such as shallow geologic units and cultural features, can be distinguished from those caused by deeper geologic units.

Automated interpretation techniques can provide information about the thickness of sedimentary basin fill, the locations of geologic contacts and faults, and the magnetic properties of buried rocks. These source parameters are important in the investigations of water aquifers, mineral resources and geologic hazards. Several experts who studied the Middle Niger (Bida) Basin recorded contradictory sedimentary pile thicknesses. Sediments from the Middle Niger Basin may extend up to a maximum depth of roughly 1000 m (Akaegbobi, 2005; Kogbe et al., 1983). Likkason & Ojo (1999) identified basic intrusive rocks at depths between 4000 m and 6000 m well below the base of the sedimentary strata of the Middle Niger Basin, based on magnetic and gravity studies. Using spectrum analysis, Udensi & Osazuwa (2004) investigated the Middle Niger basin's center and southern regions magnetically. According to their findings, the analyzed basin segment's sedimentary thickness was around 3500. Magnetism has the ability to limit quantitative details and reduce ambiguity in geological interpretation, which can lead to better identification and geological interpretation of structural structures (Farhi et al., 2016; Mohamed et al., 2020; MacLeod et al., 1993; Nabighian, 1972; Roest et al., 1992; Megwara & Udensi, 2014; Salawu et al., 2020). Geophysical method involving magnetism are commonly used in the structural interpretation of sedimentary basins because of their better spatial resolution (Li & Oldenburg, 1998).

The Anambra basin fill refers to the sedimentary layers that are found above the facies of the southern Benue Trough, and consists of lithofacies from the Campanian period to the Early Paleocene (Danian) era, resembling the Nkporo and Coal Measures Group lithofacies (Nwajide, 2013). The synclinal structure of the Anambra Basin contains a substantial accumulation of sedimentary deposits ranging from the Upper Cretaceous period to the Recent. This sedimentation phase marks the third stage of marine sedimentation within the Benue Trough, covering an area of approximately 40,000 square kilometers. The Anambra Basin connects the Benue Trough to the Niger Delta Basin, which is recognized for its enormous oil and gas deposits (Ladipo, 1988, Akande & Erdtmann, 1998).

Aeromagnetic survey had been conducted over Nigeria in recent times (2003 and 2009). These were done by Fugro Airborne Surveys on behalf of the Federal Government of Nigeria and the raw grid data in form of total-field magnetic intensity (TMI) are under the custody of the Nigerian Geological Survey Agency (NGSA). Over the confluence zones of the central Nigeria, the data were collected under the auspices of the World Bank, through the Sustainable Management of Mineral Resources Project (SMMRP). Nigeria hired Fugro Airborne Surveys (Fugro) to carry out the second phase of an airborne survey from 2007 to 2010, which covered the remaining 55% of Nigeria's land area. The TMI data obtained from the survey underwent initial processing onboard, such as magnetic compensation, verification and editing, diurnal correction, tie leveling, and micro leveling.

This work is aimed to delineate the intrusion body that controls the structural setting and formation around the river Niger-Benue confluence zone with particular attention to its solid mineral potentials, this is achieved in mapping subsurface structural features through the analysis of recent high-resolution aeromagnetic (HRAM) data-sets with the purpose of examining their effects on geological structures that characterize the confluence zones from the study area.

METHODOLOGY

Study Area

The studied area is located within 6° 00' E to 7° 30' E and 8° 00' N to 8° 30' N in the central-western half of Nigeria (Figure 1). The confluence zone (middle Niger-Benue) river (Figure 2) is presumed to be a north-westerly prolongation of the Anambra Basin (Akande et al., 2005). The sedimentary fill of the basin consists of a NW-trending belt of Upper Cretaceous sedimentary rock units which were deposited due to faulting of blocks, basement disintegration and subsidence consequent to the Cretaceous opening of the South Atlantic Ocean. The northern portion is known as the Bida sub-basin, while the southern segment is known as the Lokoja sub-basin. The Bida Formation lies unconformably on the Basement Complex in the northern part of the basin. The Lokoja Formation, which corresponds to the same geological unit in the southern part, likewise unconformably overlies the basement. The Bida and

Lokoja Formations are mineralogically and texturally young, consisting of massive, clast to matrix supported conglomerate that fines upwards to conglomeratic-sandstone, and medium grained sandstone, siltstone, and subordinate-claystone (Ojo & Akande, 2013).

The Patti Formation, which overlies the Lokoja Formation, consists of shale, sandstone, ironstone, and claystone (Ojo et al., 2020). The Bida Formation is overlain in the northern section of the basin by the Enagi Formation, which comprises of siltstone, sandstone, and claystone (Ojo, 2012). The Batati and Agbaja Formations directly overlie the Enagi and Patti Formations, respectively (Adeleye, 1974; Akande et al., 2005).

The Batati Formation is composed of oolitic, goethitic, and argillaceous ironstones with ferruginous siltstone and claystone intercalations and shaly layers, some of which produced near-shore shallow marine to fresh water fauna (Adeleye, 1973). Oolitic and pisolitic ironstones make up the Agbaja Formation (possibly Late Maastrichtian) (Ojo et al., 2020).

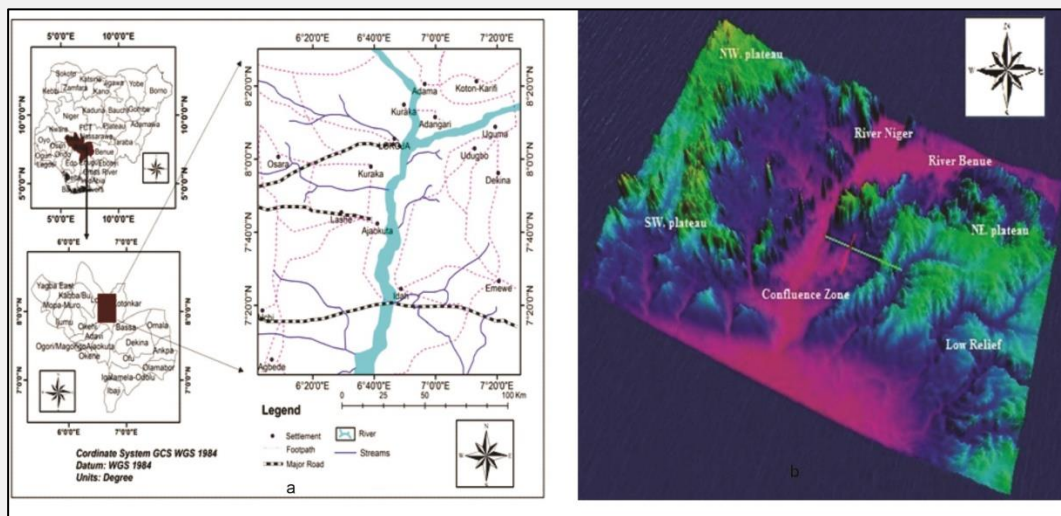


Figure 1. (a) Location map of Nigeria showing the study area (Modified from Ojabe, 2009); (b) 3D - Surface Physiography map of the study area, based on ASTER and SRTM)

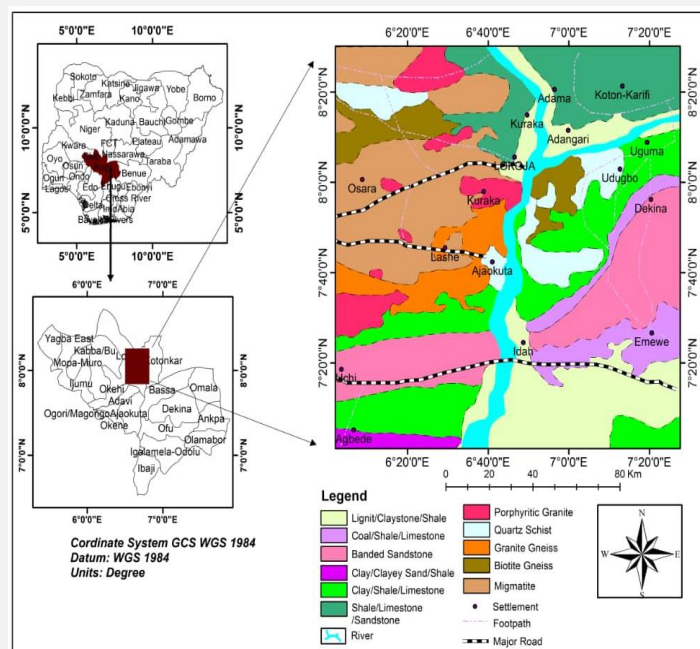


Figure 2. Geological map of the study area (Adopted from NGS, 2018)

Anambra Basin, the Afikpo Syncline, and the Niger Delta Basin were formed as a result of the tectonic movement of the axis of the Benin-Abakaliki Trough (Murat, 1972). The geological sequence of the Anambra Basin consists of the Enugu/Nkporo/Owelli Formations, which span from the Campanian to the Maastrichtian periods. During the Campanian, the Nkporo Group formations represented a shallow marine shelf, while the Enugu Shale formed poorly developed foreshores and shorefaces with extensive coastal marshes behind them. The Maastrichtian period witnessed a regressive episode, depositing floodplain sediments and deltaic foresets of the Lower Coal Measures known as the Mamu Formation.

The Mamu Formation is covered by the Ajali Formation (Obi, 2000) and is succeeded by the Nsukka Formation, which consists of fluvio-deltaic sediments (Obi et al., 2001). Obi et al. (2001) used sedimentological evidences to propose that the Nsukka Formation corresponds to a period of sedimentation characterized by fluvio-deltaic sedimentation. The Paleocene Nsukka Formation marks the beginning of another transgression, The Imo Shales, on the other hand, suggest shallow-marine shelf conditions with intermittent foreshore and shoreface sands. Blue-grey clays, shales, black shales, and bands of calcareous sandstone, marl, and limestone make up the Imo Formation (Reyment, 1965). Similarly, the Fika Shale in the Gongola Sub-Basin of the Benue Trough is composed of bluish-greenish carbonaceous shales, highly fissile shales, and occasional preserved limestones. The biostratigraphy of Cretaceous ostracods, foraminifera, and microfauna recovered from the limestone unit suggest a Paleocene age for the formation, as indicated by Reyment (1965) and Adegoke et al. (1980). The Eocene Ameki Group represents the return to regressive events.

Nwachukwu (1985) evaluated the geochemical properties of the Asata/Nkporo Shale and said it was probably deposited under a strong anoxic (euxinic) water condition. He also applied the time temperature index of loptain to evaluate petroleum prospects using the geothermal gradient model. He concluded that the Benue Trough contains only little oil formed after the Santonian event which occurs stratigraphically higher than gas. Unomah (1989) assessed the quality of organic materials in Lower Benue Trough Cretaceous shales as the foundation for reconstructing the variables controlling organic sedimentation. He inferred that organic matter and shales were deposited under a low rate of deposition.

The structural style of the Niger-River confluence zone is portrayed by a system of NW-SE trending faults at the boundaries of the basin with the surrounding crystalline basement terrain (Kogbe et al., 1983; Rahaman et al., 2018), this shows that the Middle Niger (Bida) basin is as a result of a rift. Within the sedimentary basin, no notable morphological features, lineaments, or intrusions were detected (Salawu et al., 2020). The underlying basement, on the other hand, is distinguished by prominent structural characteristics, such as the lateral continuity of the NNE-SSW trending Kalangai-Zungeru-Ifewara shear zones developed during the Pan-African orogeny (Salawu et al., 2020).

Aeromagnetic data

The Nigerian Geological Survey Agency supplied the magnetic data used in this study (NGSA). Although not publicly accessible, the Nigerian Geological Survey Agency does provide access to high resolution aeromagnetic data (NGSA). The data were obtained by a geophysical business (Fugro Airborne Surveys Limited) for the NGSA between 2004 and 2009 and are a component of the regional aeromagnetic data of Nigeria. The datasets were collected at a fixed flight altitude of 80 m over a series of NW-SE flight lines (perpendicular to regional trends). The distance between the flight lines is 500 meters, and they are connected together at a distance of 2000 meters. The major geomagnetic field component (IGRF) was removed after the data were adjusted for diurnal variation effects on board. For the purpose of analyzing the data from the aeromagnetic anomalies and determining the subsurface structural makeup of the research area, a variety of conventional digital processing techniques were used. The interpretation of prospective field data is frequently done using these techniques in order to estimate the depths and positions of structural features such intrusive bodies, contacts, and faults. Utilizing the Oasis Montaj (GeosoftTM) software suite, all aeromagnetic anomaly data processing was completed. The following procedures were used to process the magnetic data: to make it easier to understand magnetic anomalies that are affected by the directions of the magnetic field and source magnetization, the total magnetic intensity (TMI) anomaly data was turned into reduced-to-equator (RTE) data (Figure 4) (Saibi et al. 2015; Zaher et al., 2017). Remanent magnetization is typically not a limiting factor when considering the different types and ages of rocks in the area, allowing for (a) the precise application of the RTE transformation to correctly shift anomalies directly above their sources, and (b) the application of the first vertical derivative filter to enhance high frequency anomalies in order to suppress the regional effects (long-wavelength) of deep magnetic sources. As a result, we look at the magnetic patterns of

shallow source bodies, (c) apply the total horizontal derivative of tilt angle technique to enhance the magnetic signature of structures (faults or dykes), and (d) calculate the depths to the magnetic basement using the tectonic framework's spectral analysis and Euler deconvolution techniques. Below, we'll talk about the depth estimation method and enhancement filters that were used in this study.

Edge detection and depth to basement estimation techniques

An inversion process generally includes Fourier based methods which include spectral and 3D interface-based inversion (Spector & Grant, 1970) and optimization (voxel) methods (Salem et al., 2007; Werner, 1953). These inversion methods are used to invert potential field data into a 2D/3D susceptibilities subsurface spatial distribution or subsurface undulation that generate observed magnetic anomalies. Except for the voxel-based inversion approach, all of the inversion methods discussed above are used in this study. The governing equations for each approach are provided below.

Analytic signal (total gradient)

When the total gradient approach is used to analyze the observed aeromagnetic anomaly field, it typically yields accurate horizontal locations for structures (such as contacts, intrusions, faults, and sheet sources), regardless of their magnetic latitude (Phillips, 2000; Azizi et al., 2015). The magnetic direction of the source normally has no effect on the analytical signal. This causes the analytical signal to peak across the magnetic structure and have local maxima at its edges (boundaries or contacts) (Nabighian, 1972). An appealing feature for the interpretation of aeromagnetic data acquired around the magnetic equator is the lack of magnetization direction in the shape of the overall gradient amplitude (MacLeod et al., 1993). The three orthogonal gradients of the magnetic anomaly are used to calculate the total gradient (Roest et al., 1992).

$$TG(x, y) = \sqrt{\left(\frac{\partial T}{\partial x}\right)^2 + \left(\frac{\partial T}{\partial y}\right)^2 + \left(\frac{\partial T}{\partial z}\right)^2} \quad (1)$$

Where $TG(x, y)$ is the total gradient of the aeromagnetic anomaly field, the total gradient filter was used to analyze and map deeper structures over the confluence zones using the aeromagnetic anomaly data from the study area.

Total horizontal derivative of tilt angle

The total horizontal of tilt angle derivative (THDR-TDR) is produced from the tilt filter spectrum. It is used to determine the structures, trends, lithologic contact, edges, and boundaries of magnetic sources, as well as to increase both weak and strong magnetic anomalies over the studied area, this was achieved by placing the anomaly directly over its source, especially at shallow depths by using the theory that the zero contours are the edges of the formation of equation (2 and 3).

$$D = -\frac{1}{K_{max}} = \frac{1}{\sqrt{\left(\frac{\partial Tilt}{\partial x}\right)^2 + \left(\frac{\partial Tilt}{\partial y}\right)^2}} \quad (2)$$

$$THDR_TDR = \arctan^{-1}\left(\frac{1VD}{HD_{TDR}}\right) \quad (3)$$

Where 1VD is the first vertical derivative in z direction, dT/dx is the derivative in x-direction and dT/dy is the derivative in y-direction.

Improved power spectral analysis

The application of power spectral analysis to potential field anomalies in one dimension can be performed by transforming the digitized gravity/magnetic data from space domain in to frequency domain. The transformation is used to compute the power or amplitude spectrum in accordance with improved from Kebede et al. (2020) as:

$$F_{\omega} = \sum_{k=0}^{N-1} f(k) e^{-i\frac{2\pi nk}{N}} \quad (4)$$

F_{ω} is the discrete amplitude spectrum which could be respectively written as a sum of real and imaginary components as:

$$F(\omega) = a(\omega) + ib(\omega) \quad (5)$$

And with $\omega = 2\pi f$; f being the linear frequency and ω the angular frequency. The amplitude of $|F(\omega)|$ is expressed as:

$$|F(\omega)| = \sqrt{a^2(\omega) + b^2(\omega)} \quad (6)$$

The spectral analysis describes the variation of the energy as a function of frequency wavelength (Likkason, 2013).

$$h = -\frac{1}{4\pi} \left(\frac{\log E_1 - \log E_2}{K_1 - K_2} \right) \quad (7)$$

The method is a statistical estimation (Spector & Grant, 1970) based on low and high frequency anomalous bodies. These anomalies respectively categorized as sources of low, intermediate and high frequencies characteristics (Kebede et al., 2020). In this study, the profile data along the rift axis ((Figure 4), white line) is extracted from the RTE anomaly and is inverted for sources depths at various basement interfaces using power spectral analysis mentioned. The depths along the line can be calculated using Equation. (7), this approach was utilized by several researchers (Mammo, 2012) to estimate depth to basement interfaces from profile data, and the results of the analysis (depths of susceptibility contrasts) using this depth estimation method are further discussed.

Source parameter imaging

Understanding each element that characterized the sources of the magnetic anomalies is necessary for interpreting aeromagnetic anomalies. An entity that is primarily sought for is the source parameter imaging (SPI), which is a significant approach frequently used for this purpose (Smith et al., 1998). The results for the predicted depth are not affected by magnetic inclination, declination, remanent magnetization, strike, or dip (Thurston & Smith 1997). For data on aeromagnetic anomalies recorded in low magnetic latitude regions, like the study region, these qualities make the SPI technique particularly helpful. The local wavenumber ideas used by the SPI approach for depth estimate are as follows:

$$A(x,z) = \frac{\partial B(x,z)}{\partial x} - j \frac{\partial B(x,z)}{\partial z} \text{ or } A(x,z) = |A| \exp(j\theta) \quad (8)$$

Where, $|A| = \sqrt{\left(\frac{\partial B}{\partial x}\right)^2 + \left(\frac{\partial B}{\partial z}\right)^2}$ is analytical signal amplitude. According to Thurston and Smith (1997), equation (1) can also be represented as the local frequency 'f', provided by equation (9).

$$f = \frac{1}{2\pi} \frac{\partial}{\partial x} \tan^{-1} \left[\frac{\frac{\partial B}{\partial z}}{\frac{\partial B}{\partial x}} \right] \quad (9)$$

Often more convenient to re-advance as:

$$K = 2\pi f = \frac{1}{|A|^2} \left(\frac{\partial^2 B}{\partial x \partial z} \frac{\partial B}{\partial x} - \frac{\partial^2 B}{\partial x^2} \frac{\partial B}{\partial z} \right) \quad (10)$$

Thus:

$$h = \frac{1}{K_{max}} \quad (11)$$

The work is started by calculating the grids as $\left(\frac{\partial B}{\partial x}, \frac{\partial B}{\partial z} \text{ and } \frac{\partial B}{\partial y}\right)$. Therefore, maximal values of K are found above the sloping contact in the 2-D slope contact model that SPI adopts. Additionally, the depth values of magnetic sources are calculated by inserting equation (2) into the following expression in Eq. (3) for the depth estimate:

$$\text{Depth} = 1/K_{max} \quad (12)$$

Where K_{max} in equation (12) refers to K_{max} 's greatest value above a 2-D sloping contact (equation 11). To determine the depth values of sources inside the basin and its surroundings, the local wavenumber technique was applied to the aeromagnetic data of the Niger-Benue river confluence zone and its surroundings. This is done in order to determine the depth of the basin's sedimentary layer and the range of depth values of the sources inside the basement terrain nearby.

Euler deconvolution techniques

It is common practice to use Euler de-convolution (ED) to extract the geometry of causal entities from potential field data. Hood used this technique to analyze aeromagnetic data and showed that it is appropriate for sources that are pointed dipoles and point-poles. A potent method for determining depth directly and interpreting likely source geometry is the Euler De-convolution. The technique may pinpoint or sketch constrained sources, dykes, and contacts with astounding accuracy.

Werner deconvolution techniques

Werner (1953) introduced the mathematical definition of 2D Werner deconvolution, which was followed and extended by Hartman et al. (1971). As a result, for simple arbitrarily oriented thin sheets (dykes) or interfaces, the governing equation of a total magnetic field is given by;

$$F(x) = \frac{Ah+B(x-x_0)}{(x-x_0)^2+h^2} \quad (13)$$

For the more complex model, the anomalous magnetic field is regarded as:

$$F(x) = \frac{A_1h_1+B_1(x-x_1)}{(x-x_1)^2+h_1^2} + \frac{A_2h_2+B_2(x-x_2)}{(x-x_2)^2+h_2^2} + c_0 + c_1x + c_2x^2 \quad (14)$$

Where x is the distance along a line perpendicular to the thin sheet's strike relative to an arbitrary origin; $F(x)$ is the total magnetic field strength at x ; h is the depth to the thin sheet's top; and x_0 is the top's location projected vertically to cross the line. A and B are parameters relating to the magnetic characteristics, thickness, and orientation of the thin sheet relative to the direction of the Earth's field. The anomalous magnetic field is regarded to be the combination of the fields owing to two thin sheets plus a quadratic background magnetic interference in the more sophisticated model, which may be represented as (equation 15).

$$A_1; h_1, B_1, x_1; A_2, B_2; h_2; x_2; c_0; c_1 \text{ and } c_2 \quad (15)$$

The first eight variables are vital to the interpretation, and it is solved analytically. The model equations are solved using observed data values, yielding the position, depth, and magnetic contrast of buried interfaces. To solve for these unknowns at one point on the profile, a 'window' of 11 equi-spaced observed data values is required. Solving these systems of equations results in estimates of these coefficients, and allows one to determine the position and depth of thin-sheet bodies as well as geological interference. This approach is an automated inversion method that does not require any prior knowledge, and provide a 2D representation of the distribution of subsurface point sources coefficients. In this study, RTE magnetic anomalies along rift axis (Niger – Benue confluence zones) are first extracted respectively from gridded magnetic anomaly maps. These profile datasets are subjected to the Werner method in order to calculate the relevant depths to magnetic source interfaces. Different scholars employed the technique in various study areas to determine the depths of gravity and magnetic sources (Mammo, 2012).

2D forward modeling

It explains the method of creating synthetic data from an original Earth model that has geometric components and physical characteristics (Menke, 2018). For the case of an n-sided polygon, Talwani et al. (1959) divided the line integral into n-contributions, each of which was connected to a different side of the polygon. Talwani et al. (1959) developed equations for z_i that extensively reference trigonometric functions. The model entails developing a hypothetical geologic model and computing the earth's magnetic reaction. In this work, the profile magnetic response with changing susceptibilities and undulating layer geometries is calculated using the intuitive, interactive, and real-time GM-SYS modeling application from Oasis Montaj Geosoft. Since this modeling approach is not unique, it must be limited by the geological and geophysical knowledge that has been accumulated over time. This method has been a recognized procedure for determining the profile geometries of interfaces (Talwani et al., 1959).

RESULTS

The lithologies and structures of the research area were delineated and characterized using Power Spectral Analysis, 2D Euler, and Werner De-convolution, and the total magnetic intensity map was analyzed and interpreted.

Total Magnetic Intensity (TMI)

A positive magnetic intensity value of up to 33168.28 nT is seen on the total magnetic intensity map (Figure 3), which dominates the east-west direction with a small section in the southeast of the research area. In the east-central region, it was discovered that the high magnetic intensity varied by moderate magnetic intensity (33115.41 to 33146.52 nT). The Dekina-Lokoja-Kabba areas have a high magnetic intensity, while the Ejule area has an intermediate magnetic intensity.

The intermediate magnetic intensity dominates the east, west, and southern portion of the research area. These regions were identified as minor intrusive bodies, which are made up of shale, limestone, and sandstone. Fairly low magnetic response (32888.10 to 32975.52 nT), and low magnetic intensity (32981.95 to 33022.43 nT) were found at the northern portion of the map. These characteristics were thought to be the River Benue Group's carbonaceous shell. The northeastern portion of the map exhibits a dome shape in the same trend direction, while the northwestern portion of the map has low magnetic intensity responses. There are low magnetic signatures observed to vary between (33048.29 to 33115.40 nT) and intermediate magnetic intensity (33032.98 to 33048.29 nT) at the southern and western portions of the map, respectively. As can be seen on the map (Figure 3), both the low and intermediate magnetic intensities coincide with the shell and limestone over the confluence zone. Faults are shown at the north to the central region, demonstrating the dome shape and the two main trends, NE - SW, and E - W.

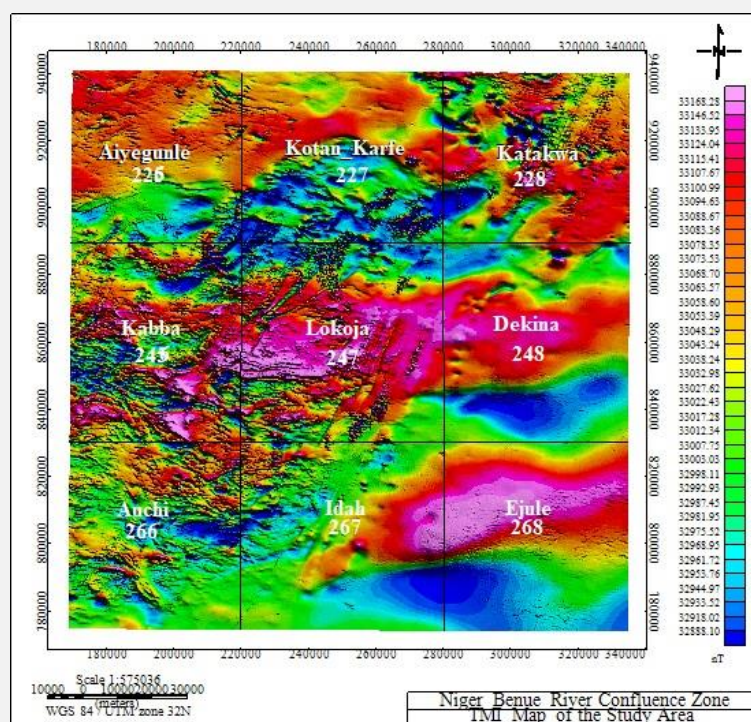


Figure 3. Total Magnetic Intensity (TMI) Image of Niger – Benue River Confluence Zone

Source Parameter Imaging (SPI), 2D Euler and Werner De-convolution, Power Spectral Analysis, and the estimated magnetic source depths along the rift axis of the confluence zone are all mathematically formulated.

Reduced-to-magnetic equator (RTE) map

The resulting magnetic anomalies are a reflection of the magnetic signatures found in the basement and intrusive rock units in the research area (Ojo & Akande, 2013). These structures were identified using the RTE magnetic anomaly map, which had signatures that aligned with the causative bodies. The RTE-anomaly map's visual examination is shown in Figure 4.

The reduction to magnetic equator (RTE) of the crustal field anomaly map (Figure 4) reveals positive and negative magnetic intensity values up to 164.42 nT, which dominated the southwest corner of the research area. The southern section exhibits similar features that strike in a NE-SW orientation.

Rocks with intermediate to high magnetic intensities predominate in the central part of the study area. Over the confluence zone, the River Niger Group correlates with values of intermediate to high magnetic intensity.

Figure 4 depicts variations in magnetic intensity that might be related to variations in the mineral makeup of the rocks in the study area. The relatively low magnetic intensity (-84.31 to -20.45 nT) that dominates the northern section of the map can be interpreted as the shale, limestone, siltstone, and carbonaceous sandstone within the river Niger. This feature is also visible in the northwest and southeast regions of the map, both of which exhibit a trend in an approximately NW - SE direction. The body, with a magnetic intensity ranging from 30.89 nT to 102.23 nT, is classified as a minor intrusive body and is located in the southern region of the map, where the trend is from south to west. The ferruginous elements were observed to be correlated with the high magnetic intensity and a low magnetic intensity (-198.66 nT to -103.76 nT) response striking virtually eastward is observed in the northern section of the region. This weak magnetic field is associated with the carbonaceous shale in the Niger River. Three faulting systems (Anka, Yauri, and Iseyin) were identified, having NE-SW, E-W, and NW-SE patterns, as shown on the map (Figure 4). According a study, the variations in fault patterns were caused by the earth's crust's deeper heterogeneity during the series of events that led to the opening up of the South American and African plates.

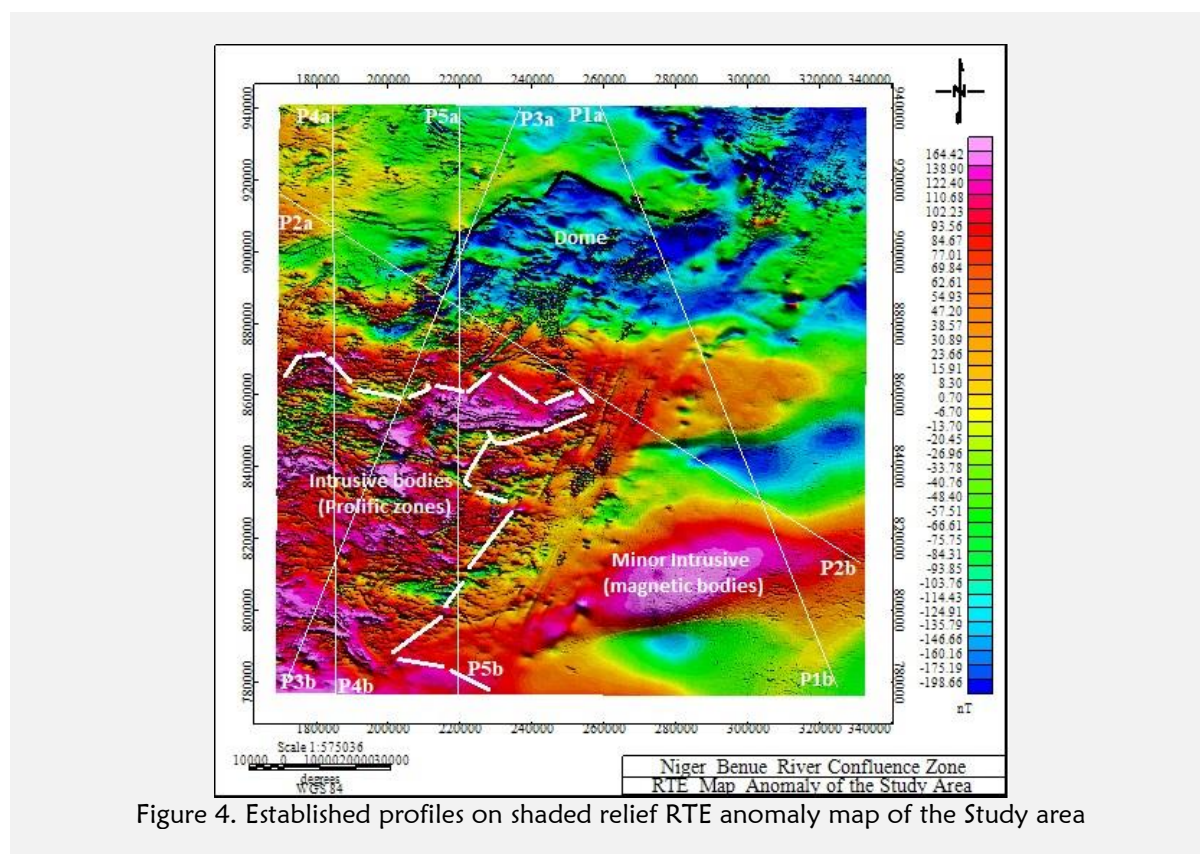


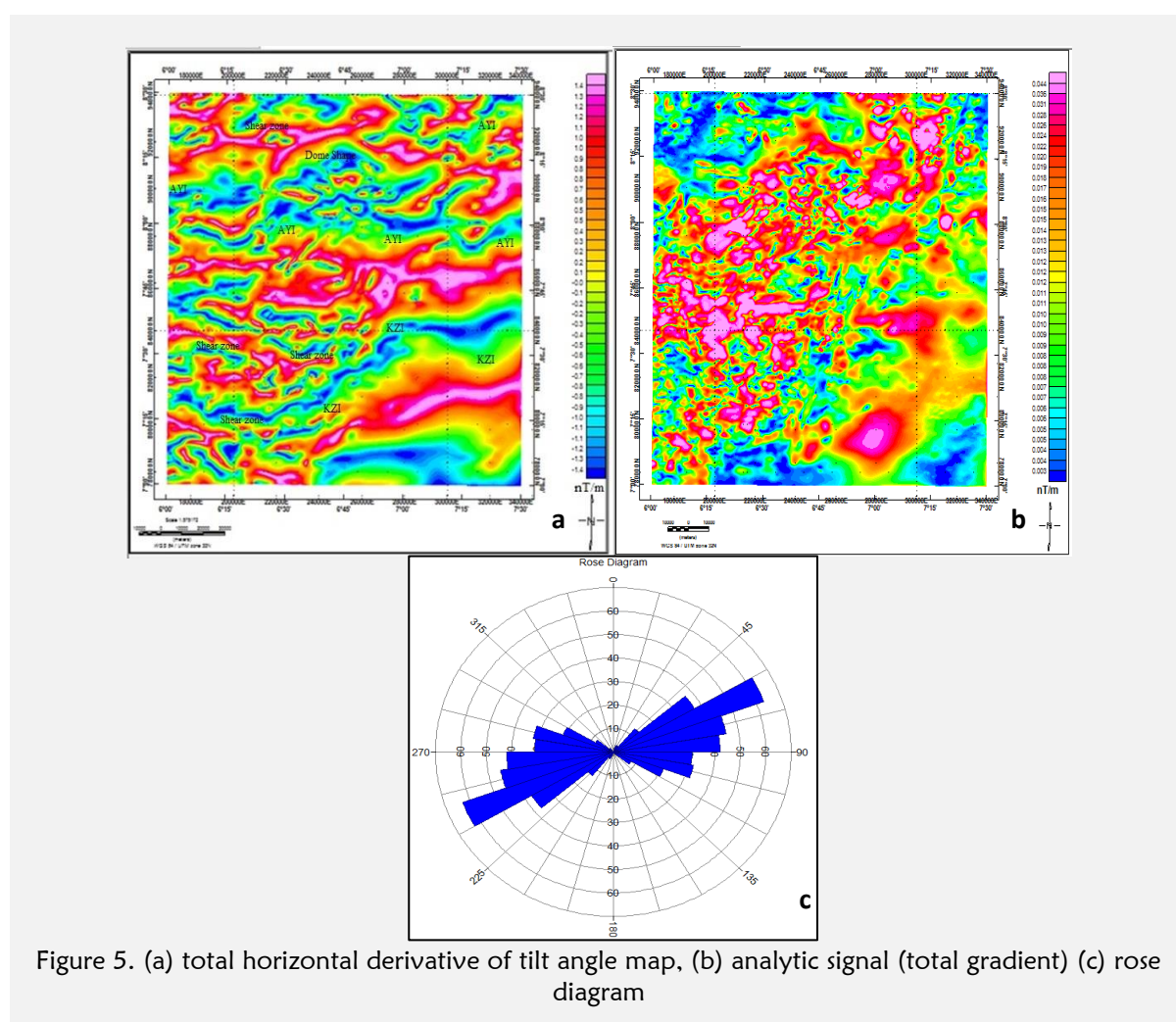
Figure 4. Established profiles on shaded relief RTE anomaly map of the Study area

Structural features over the Niger – Benue river confluence zone based on edge detection

To identify potential mineralized targets, the zero-contours of TDR and total gradient (analytic signal) often sharpen the locations of magnetic source contacts and edges and trace shallow geological formations (Salem et al., 2007; Hood, 1965). The mineralized sites are located in areas with high magnetic anomalies and almost at the zero contours of TDR, i.e., where the magnetic susceptibility of rock unit varieties and/or geological structures take place, according to TDR-maps (Figures 5a and 5b), which superimpose the locations of the confluence zone over the total gradient (analytic signal).

These results would suggest that the structural system played a substantial role in the mineralization of the western regions of Koton-karfe, Lokoja, Kaba, and Ida. The rose diagrams of the zero-contours of the TDR-map show that the NNE-SSW and WNW-ESE (respectively) are the dominant structural trends (Figure 5c). On the analytical signal map (Figure 5b), the gradient values vary from 0.0051 nT/km to 0.3812 nT/km. It is anticipated that positive anomalies will be associated with

surrounding mineralized bodies and/or rock units that have a high magnetic susceptibility (example: serpentinite, metavolcanics, and granitic intrusions). The reduced-to-equator magnetic and tilt of angle derivative (TDR) map (Figure 4a) shows a rough relief and anomalies with amplitudes ranging from -0.162 to 0.189 nT/m, both positive and negative. The primary magnetic trends in the basin and its surrounding crystalline foundation complex are in the directions of NW-SE, N-S, NE-SW, and E-W. In the basement terrane, extended regional gradients with NNE-SSW trends are connected to the Anka-Yauri-Iseyin (AYI) shear zone to the west and the Kalangai-Zungeru-Ifewara (KZI) shear zone near the Zungeru area. The Campano-Maastrichtian ironstones, which have been previously studied by Ojo & Akande (2013) and Ojo et al. (2020) create a number of magnetic minerals that are responsible for the low amplitude magnetic anomalies inside the basin, which extend from Bokani via Bida to Abaji regions. This suggests that the sedimentary layers of the basin's basin may not include any volcanic materials. These elongated, low-amplitude magnetic anomalies primarily trend in the north-south and east-west directions. On both the total gradient and TDR maps, a few elongated low amplitude magnetic anomalies with NE-SW patterns can be seen in the basin's middle region. In their comprehensive analysis of the southern Middle Niger Basin, Ojo & Akande (2013) found that the Lokoja Formation contains heavy metal mineral assemblages like magnetite, hematite, limonite, and ilmenite. The Nigerian confluence zones and their surrounding crystalline basement area provide a magnetic signature that is generally visible on the TDR map.



Depth Estimation to buried magnetic sources Radially averaged power spectrum (RAPS)

The average depth of source assemblages can be determined using the power spectrum, a 2D function of energy and wave number (Spector & Grant, 1970). The entire depth estimates to the top of the magnetic sources that created the detected anomalies in the research area is shown in the radially

averaged power spectrum or spectral plot (Figure 6). Based on the wavelength of the magnetic sources, the layers' gradient was determined. The gradients of the shallower and deeper magnetic sources are 1.60 km and 4.47 km, respectively. As a result, the total depth estimations to the top of the magnetic shallower and deeper sources in the region are 0.82 km (815.1 m) and 2.25 km, respectively.

Spectral depth analysis

Figure 4 depicts the five profiles of the shaded relief reduce-to-magnetic equator anomaly retrieved along the rift axis across the Niger-Benue river confluence zone. The one-dimensional power spectrum approach is used to analyze RTE anomaly profiles using 144 data points from spectral blocks. The power spectrum curve calculated is expressed as the log of spectral energy vs wave number. The slope (gradient) of the power spectrum curve is used to compute the depth to top and shallow of the magnetic source (deep and shallow interfaces). A piece-wise least-squares linear curve fitting technique is used to fit linear curves (from which slope values are read) to power spectral data. The gradients (slopes) are calculated from the fitted lines, which represent the weighted energy of the source origin at low and high frequencies. Much of this energy originates from low-frequency sources (Figure 6(a-f)). Table 1 summarize the power spectral analysis results depending on the wave number (frequencies) and slope (gradient) changes, source depth interfaces are classified as shallow or deep.

The depth to weak magnetic sources across the rift axis of the confluence zone is approximately 1.5 km, while the depth to deep magnetic sources is 4.7 km. As the method is used to determine mean depths to the various interfaces of magnetic contrasts, two clearly identified interfaces are read and classified as deep and shallow source depths (Table 1). Figure 7 shows a map of the magnetic horizons across the study area. The shallow interface depth is calculated to be approximately 23 m, with a r^2 value of 0.0002. Accepting 23 m as a source depth with an r -square value may result in an incorrect interpretation. As a result, it is preferable to think of it as terrain clearance effects. The structural maps (Deep and Shallow) yielded in mapping the magnetic horizons across the study area were produced using the source depth estimate approach (Figure 7).

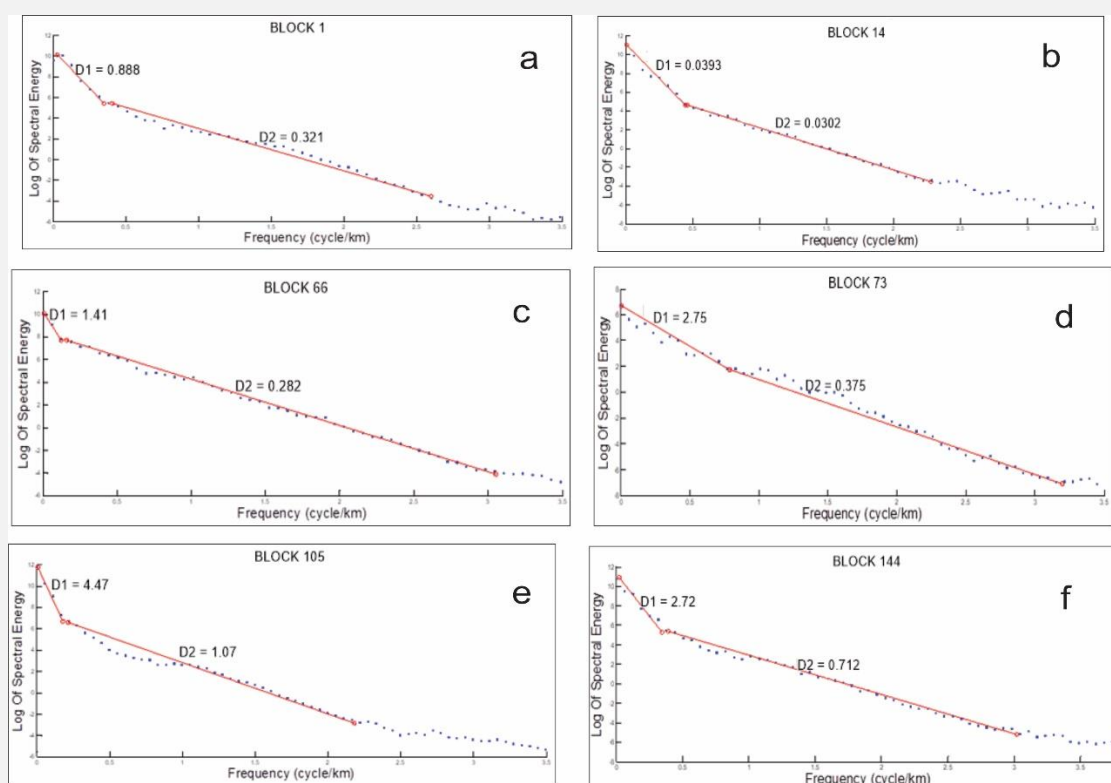


Figure 6. (a-f) An example of spectral plots over the Niger – Benue river confluence

Table 1. Log spectral depth estimates and category of the anomalous source as deep and shallow components

Depth (Deep) (km)	Depth (Shallow) (km)	Depth (Deep) (km)	Depth (Shallow) (km)
0.888	0.321	0.805	0.656
0.654	0.409	0.677	0.275
0.374	0.297	0.403	0.374
0.498	0.342	0.458	0.296
0.725	0.61	2.4	0.412
1.56	0.788	1.42	0.623
0.916	0.725	1.12	0.354
0.661	0.409	1.46	0.316
0.486	0.414	1.08	0.404
0.672	0.43	0.772	0.514
0.575	0.343	1.87	0.532
0.597	0.264	1.24	0.374
0.553	0.359	2.43	0.661
0.0393	0.0302	1.47	0.303
2.86	0.274	1.68	0.504
0.678	0.312	1.53	0.517
1.04	0.425	0.81	0.299
1.43	0.743	1.39	0.51
1.43	0.915	0.807	0.159
1.68	1.53	2.75	0.391

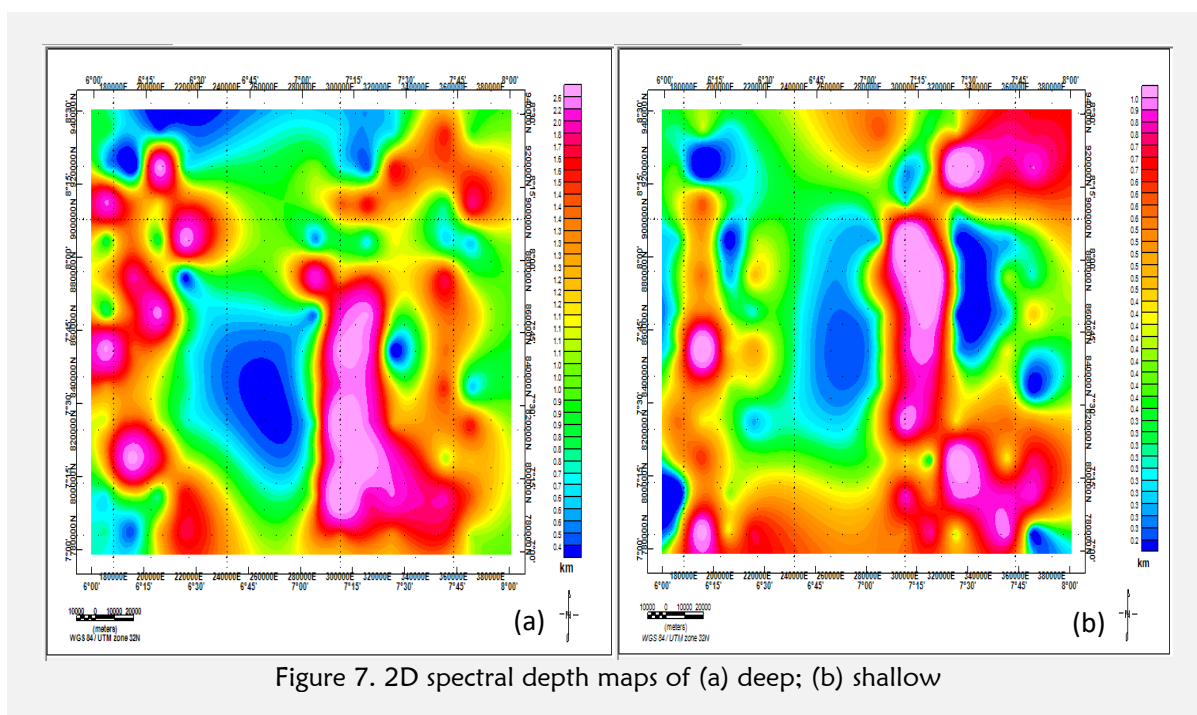


Figure 7. 2D spectral depth maps of (a) deep; (b) shallow

Improved source parameter imaging

The Nigerian Basement, which contains remnants of the Pan-African tectonic event (600 Ma), underlies and surrounds the Niger –Benue river confluence zone. Dominant southeastern shears define the principal structural fabrics (foliations, lineations, folds, etc.) of the entire region (Dada, 2008). Applying the imaging of the local wavenumber technique is one way to determine the depth to the top of sources (such slope contact and thin sheet models). These estimates can be used to depict the morphology of the basin floor, which is directly related to the region's structural history. The SPI map (Figure 8) shows the estimated depths of sources in the investigated area, which range from 593.7 m to

9968.0 m. 3286.1 m is the average depth value related to penetrative structural elements within the crystalline basement complex terrain. The higher and constant depth values of the entire research zone, which includes Ejule, Dekina, Lokoja Koton-karfe, and Auchi, in contrast to the lower depth values of the nearby basement complex areas, is a particularly eye-catching aspect of the map. Figure 8's pattern of depth values enables visual evaluation of the SPI map with the borders of the Confluence zones (which are indicated by the end of structural features) on the structural map (Figure 8). The interior geometry of the research region is represented by the constant depth values of 2937.1 m.

To further separate the basin from the surrounding basement terrain, the SPI map's coverage of the Niger-Benue confluence zone was excised. To create a sedimentary thickness map of the basin, the value of 837.6 m sensor mean terrain clearance was subtracted from the resulting region SPI map (Figure 8). The estimated thickness of non-magnetic geological material above the magnetic basement is shown on the map.

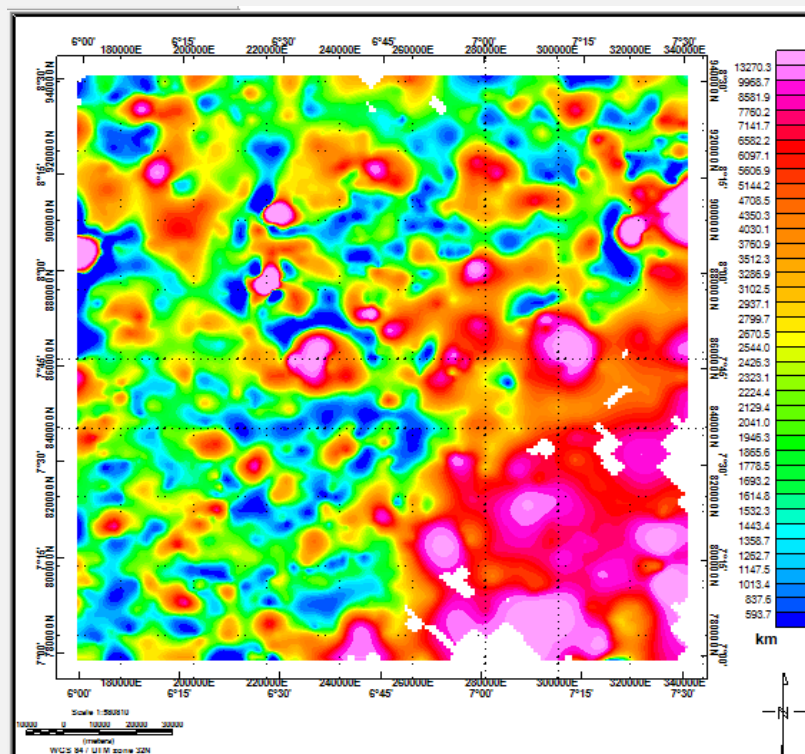


Figure 8. local wave number (SPI) anomaly map

Euler depth solution

Euler depth estimation was applied at shallow depths (0 – 150 m) using structural index (SI) of 0 and 1 (Fig. 9a and 9b). The map of structural index (SI) = 0 (Fig. 9a) reveals the depths of the magnetic contacts (< 4000 m). Some of them extend deeper to reach about > 1000 m depth. The lineament trend of these magnetic contacts shows the NNW-SSE and NNE-SSW trends as the main trends and the NWSE and NE-SW trends as the secondary trends. The known pits over the Niger – Benue river confluence zone are located directly over these contacts. Meanwhile, the structural trends of the dyke solution with SI = 1, shows that the NNESSW and NNW-SSE trends, respectively, are the dominant trends of magnetic dykes and faults (Fig. 9b). In addition, Euler depths were calculated for deep sources using limited depth results (< 5000 m) for SI = 0 and limited depth results (5000–10000 m) for SI = 0 (Fig. 9b). These constraints were used to investigate the extended roots of various magnetic sources. The structural lineament of these maps exhibits roughly the same patterns as shallow magnetic sources, indicating that these sources have deep-rooted extensions. Critical evaluation of the depth maps produced reveals that Ejule and Dekina represent deep-rooted sources at depths ranging from 500 to 2500 m (Figure 8), whereas Aiyegunle, Lokoja, and Kabba indicate deep-rooted contacts/faults at around 600 m (Fig. 9a). The copper mine is located on top of deep dykes/sills that range in depth from 5000 to 25000 meters (Figure 9b).

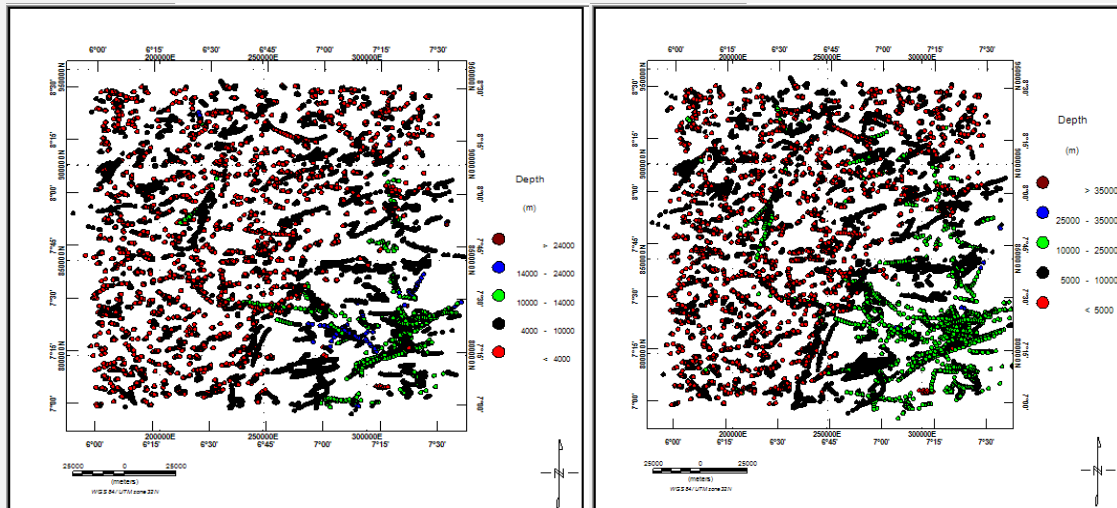


Figure 9. Euler depth solution (a) (Contact_-0.5, 1 SI); (b) (Dyke_0, -1 SI)

Werner depth solution

The magnetic source depth and location across the rift axis of the Niger-Benue river confluence zone are also computed using Werner De-convolution, an automated depth-estimation approach. The governing equation that aids in depth estimation is presented in the preceding section. This approach is an iterative 2D inversion technique that calculates the depths and positions of vertical magnetic sources. The RTE anomaly along the confluence zone rift axis is first derived from the RTE anomaly map (Figure 4). The Werner technique is used to this profile anomaly in order to extract magnetic source vertical contact depth positions. Figure 10 (a-e) depicts this using square symbols.

Similarly, the magnetic anomaly that is differentially reduced to the equator along the same profile line as the magnetic profile is retrieved and subjected to the Werner magnetic profile depth method. Figure 10 (a-e) depicts the outcome of magnetic source depth. The trend line fitted to this elevation profile has a negative slope, indicating that the height tends to drop northwards. The magnetic source depth calculated using the Werner automated inversion technique appears to deepen northwards, as seen by the fitted trend line to the magnetic source depths. Magnetic source depths appear to deepen from south to north, similar to the magnetic source and elevation patterns (Figure 10 (a-e)).

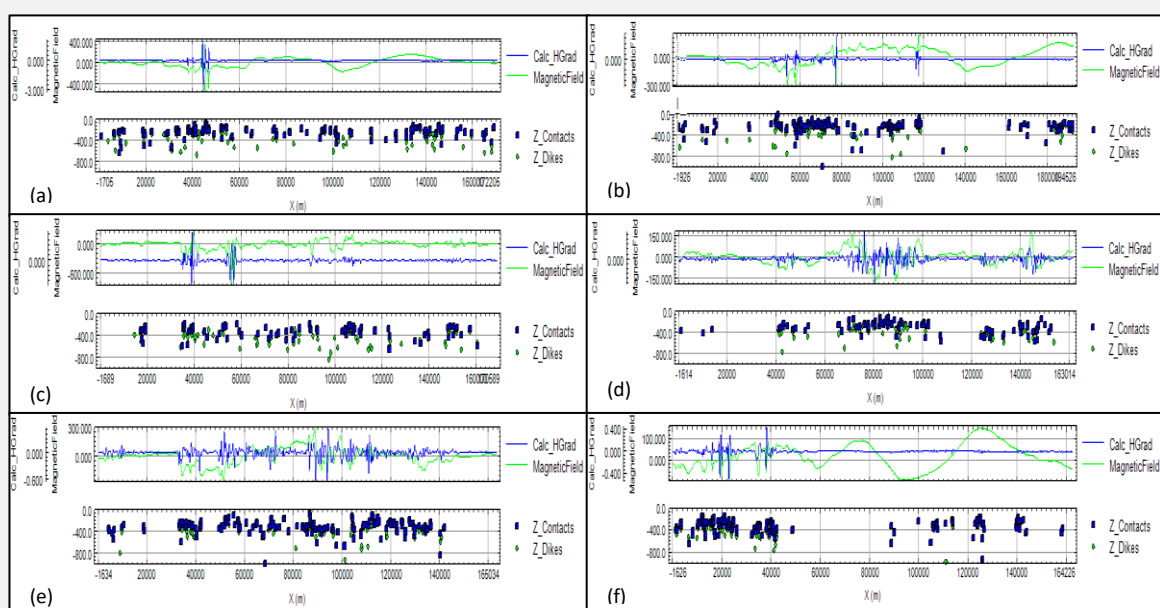


Figure 10. (a-f) Werner depth plot solution extracted from path of the six established profiles

Two-dimensional magnetic forward modeling and structural inversion across profiles 1, 4, and 5

When the independently generated 2D spectral depth values were compared to the magnetic models across the selected profiles, the latter were found to better represent the geology of the research area (Figure 6(a-f)). Based on the initial constraining data mentioned in Table 1, the 2D joint magnetic model is calculated using the reduced to magnetic equator profile (Figure 4). The basic model consists of six lithologic strata, including basement, post-rift sediment, alluvium, shale/limestone/clay, sandstone/clayey-sandstone, and sandstone (Table 1 and Figure 6). The final magnetic model response is assumed to be acceptable, with a root mean square error (RMSE) of 0.02161 nT and 84.67 nT, respectively (Figure 4). The observed and computed magnetic anomalies along the profile fit well with this combined model. Figure 11 (a-c) illustrates how the thickness of the sediment-infill grows as one moves farther north, covering the Niger-Benue river confluence zone.

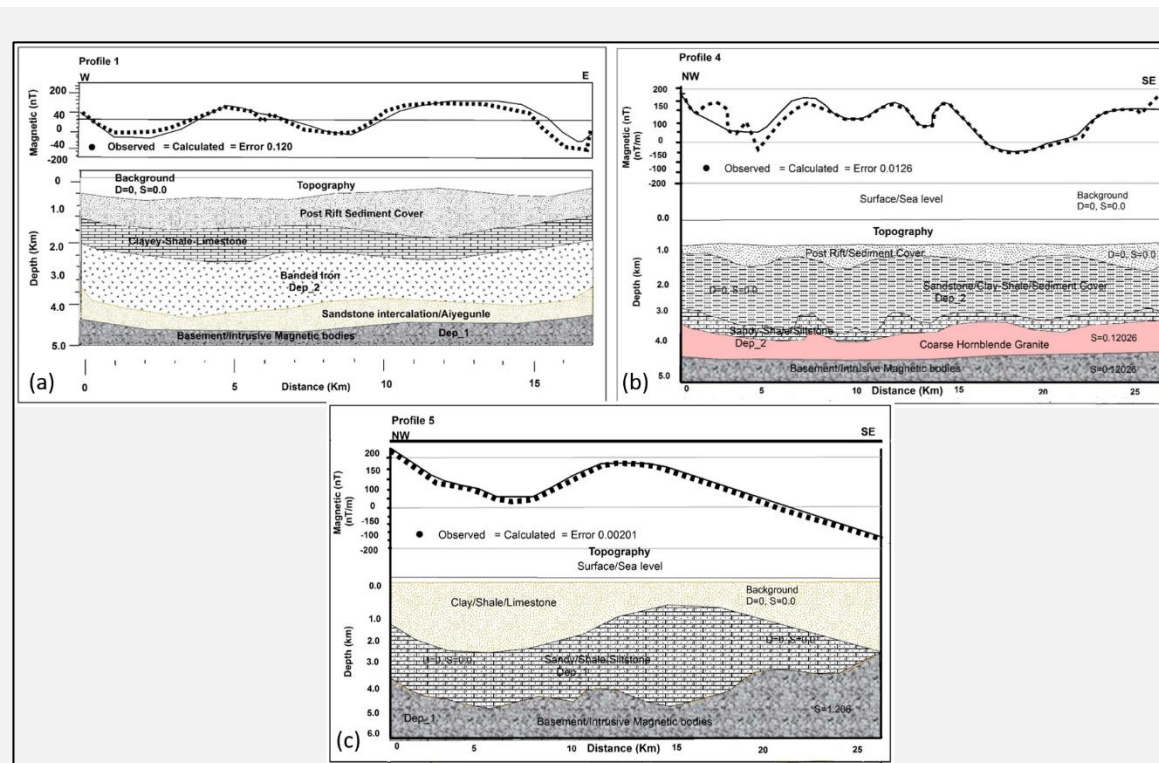


Figure 11. (a-c) 2D magnetic forward model of the profile running along the rift axis and rift floor, considered to show the magnetic horizons. The deeper crystalline basement sources overlying shallower sedimentary sediment filling sources.

Despite the fact that the sediment-in fill layer was very lightly mapped, this result is in good agreement with other researchers' publications. These depth estimations from the 2D magnetic modeling are in agreement with the automated depth-to-source calculations done with the help of spectral analysis, 2D Euler deconvolution, and source parameter imaging techniques. A number of surfaces or geologic horizons are inverted in the 2D forward and inverse modeling approach to map the anticipated depth to layers (Figure 11(a-c)). The residual reduced-to-equator magnetic anomaly is transformed to basement depths using the Parker-Oldenburg algorithm's multi-layer, surface-based, frequency domain forward and inverse modeling technique. This inversion needs a priori data from already completed geological and geophysical research (Table 1, Figure 2). It is done for layer geometries (litho-stratigraphies) in general and basement layer depth in particular. In light of this, the inversion is performed on the basement's surface using a 3-kilometer reference depth. The settings for the lowest and highest cut-off frequencies are chosen to be 0.03 and 0.05 km⁻¹, respectively. After four (4) iterations, the structural inversion performed on the basement layer is determined to have converged. From the structural inversion, the corresponding calculated and misfit RTE anomalies are created for the calculated topographic relief (Figures 11 a, b, c). Figure 11c shows the shallow depth to the foundation top layer map at 0.8 km and the deeper top depth map at 4.5 km. These are 800 meters above and 1.5 kilometers below a reference depth of 5 kilometers along the rift axis, particularly beginning north of Ejule, Dekina, Lokoja, Koton-

Karfe, and Auchi. The depth of the magnetic source appears to be very deep. Additionally, it has been noted that the magnetic basement fabric is deepening northward toward the Benue trough. For comparison with the current result, the area has undergone previous shallow or intermediate depth geophysical studies. The outcome is somewhat consistent with the 2D Werner deconvolution, SPI, and combined 2D magnetic modeling results from this study. Despite being mapped with low resolution, the depth analysis study carried out in the region by other researchers shows shallow sediment filling tends to deepen northward (Ojo et al., 2013), in conformity with the outcome of the 2D model.

DISCUSSION

Subsurface structures

Several inversion approaches were employed in this work to gain a better understanding of a variety of susceptibility interactions. The geometry of these susceptibility layers is intimately tied to the margins of geological formations (Telford et al., 1976; Feng et al., 2016). The method employs power spectrum analysis, 2D Euler and Werner de-convolution, source parameter imaging, 2D forward modeling, and interface inversion techniques to pinpoint the causes of magnetic anomalies. The first inversion approach used in this work to locate the origins of magnetic anomalies occurring along the rift axis of the Niger-Benue confluence zone is power spectral analysis. The slopes of lines fitted to plots of a log of power (energy) vs. wave number are calculated as part of the research (Figure 6(a-f)). These slope values, computed in line with equation (6), are used to estimate the depths of the magnetic source along the profile under discussion. The magnetic sources detected at such a shallow depth (1.53 km) are considered to correlate to the tops of the following rock types: Aiyegunle (Biotite and Biotite Hornblende Granite), Kotan-Karfe (Feldspathic Sandstone and Siltstone), Katakwa (Fine-grained Flaggy Quartzite and Quartz Schist), Kabba (Migmatite), and Lokoja (Porphyroblastic G) (Figures 2 and 3). The top of the basement depth (3 km), which was recognized by the magnetic source having a deeper origin along the profile, was discovered nearby at a depth of 4.47 km (Likkason & Ojo, 1999).

Secondly, the depth to the top of the magnetic source interfaces along the rift axis of the Niger-Benue river confluence zone is determined using 2D Werner de-convolution of the reduce-to-magnetic-equator anomaly (Figure 10(a-e)). The low "sediment-volcanic" layer over the confluence zone is predicted to deepen from south to north according to trend lines fitted to Werner's estimated magnetic source depths.

The imaging source parameter is the third filter that is used to map source depths (SPI). The "lithostratigraphic" layer covering the basement strata over the confluence zone is thickening northward, according to the analysis of SPI of magnetic data. This indicates that the low magnetic source bodies' (sediments') thickness rises toward the north. In other words, the northern part of the study area has much deeper crystalline basement rock strata than the southern part.

The SPI symbol depths magnetic map (Figure 8) reveals that shallow magnetic sources are more easily identifiable than deep-seated targets. The majority of these shallow magnetic sources are represented in (Figure 7b), with depths ranging from 1.1 to 2.6 km. The deepest depth zone designated by "A" (Figure 7b) has a maximum depth of about 4.7 km. According to the depth distribution symbols map (Figure 7b), the most common (concentrated) depth location for magnetic source bodies in the region is between 1 km and 3 km.

The magnetic source depth estimated from SPI along the over the confluence zone mostly agreed with low magnetic signatures amplitude response identified by Likkason et al., (2013). The result from analysis of SPI agrees with the 2D Werner De-convolution results obtained from magnetic data. According to the SPI symbol depth magnetic map, shallow magnetic sources can be found more readily than deep-seated targets (Figure 8). The majority of these shallow magnetic sources are seen in (Figure 7b), with depths ranging roughly between 1.1 km and 2.6 km. A rough maximum depth of 4.7 km can be found in the deepest depth zone labeled "A" (Figure 7b). We can see from the depth distribution symbol map in Figure 7b that the most frequent (concentrated) depth location for magnetic source bodies in the area is between 1 and 3 kilometers deep. The low magnetic signature amplitude response discovered mainly agreed with the magnetic source depth determined from SPI over the over the confluence zone by Likkason et al. (2013). Both the 2D Werner De-convolution results and the outcome of the SPI analysis are in agreement.

CONCLUSION

The geologic boundaries and edges of tectonic features are superimposed, revealing that the majority of mineralized zones are located over edges, indicating structural control of mineralization

origin in the east-west Niger-Benue river confluence zone. This information was obtained using the zero contours of TDR, FVD, total gradient (analytic signal), and Euler maps. While residual magnetic bodies and surface lineaments in remote sensing data follow the NNE-SSW and WNW-ESE directions, the prominent structural trends of deep sources stretch mostly in the NE-SW and NW-SE directions. This suggests that rocks may have rotated after the first revolution. Such movement-induced deformation may result in surface and near-surface mineralization. The circular features of the late-to-post tectonic granitic intrusions were sharper, while the elongated metavolcanics and serpentinite belts faded with depth, according to a correlation between the geological units east to west of the confluence zone and the magnetic data. This may imply that serpentinite belts and metavolcanics are allochthonous blocks with no roots. Different rock units and alteration zones can be successfully identified using topography, especially over the study area and along the extreme borders in general. This study used potential field data to determine the depth of magnetic source bodies in the zones of the Niger Benue river confluence. To understand lithological layer geometries better, automatic inversions of 2D magnetic forward modeling and structural inversion are used. Using the aforementioned mathematical techniques, horizons showing magnetic source depths are calculated. Using power spectral magnetic depth analysis, two source depths of 1.60 km and 4.47 km were determined. The source depths in the 2D Euler and Werner deconvolution analyses of magnetic data are deepening southeast, according to the fitted trend line to the geometries in vertical contact. Similarly, the SPI method depths to magnetic sources range from 593.7 m to 9968.0 m and are thought to demonstrate the thickening (deepening) of the shallow overburden. Furthermore, the 2D Werner deconvolution and SPI results are consistent with those of the 2D magnetic forward modeling. The three-layer earth model is used to classify the shallow overburden layer referred to as "sediment-volcanic" in this study. The combined interface geometries mapped using the various filtering procedures are closely congruent with one another and with the region's preexisting a priori geological and geophysical information. In accordance with the findings of the rose diagram study, the shallow "sediment-volcanic" layers that were identified using magnetic data also seem to deepen northward. It is believed that the structures (topographic layers) that were mapped in this study control the inter-basin structural features and dynamics of the study area.

ACKNOWLEDGEMENT

The high-resolution aeromagnetic data and digital elevation model (DEM) for this research were bought from the Nigerian Geological Survey Agency (NGSA), Abuja. I would like to offer my sincere gratitude to two staff members of the Nigerian Geological Survey Agency (NGSA), Abuja, for their assistance in the assembly and treatment of the nine aeromagnetic sheets as well as for providing me with the knowledge and insight that considerably aided my study work.

REFERENCES

- Adegoke, O. S., Ako, B. D., & Enu, E. I. (1980). *Geotechnical Investigations of the Ondo State bituminous sands Vol. 1. Geology and Reserves Estimate*. Unpub. Rept., Geological Consultancy Unit, Department of Geology, University of Ile-Ife, 257pp.
- Adeleye, D. R. (1973). Origin of ironstones, an example from the middle Niger Valley, Nigeria. *Journal of Sedimentary Research*, 43(3), 709-727. <https://doi.org/10.1306/74D7284C-2B21-11D7-8648000102C1865D>
- Adeleye, D. R. (1974). Sedimentology of the fluvial bida sandstone (cretaceous), Nigeria. *Sedimentary Geology*, 12(1), 1-24. [https://doi.org/10.1016/0037-0738\(74\)90013-X](https://doi.org/10.1016/0037-0738(74)90013-X)
- Akaegbobi, M. I. (2005). Sequence Stratigraphy of Anambra Basin. *Journal of African Earth Sciences*, 42, 394-406.
- Akande, S. O., & Erdtmann, B. D. (1998). Burial metamorphism (thermal maturation) in Cretaceous sediments of the southern Benue Trough and Anambra Basin, Nigeria. *AAPG bulletin*, 82(6), 1191-1206. <https://doi.org/10.1306/1D9BCA39-172D-11D7-8645000102C1865D>
- Akande, S. O., Ojo, O. J., Erdtmann, B. D., & Hetenyi, M. (2005). Paleoenvironments, organic petrology and Rock-Eval studies on source rock facies of the Lower Maastrichtian Patti Formation, southern Bida Basin, Nigeria. *Journal of African Earth Sciences*, 41(5), 394-406. <https://doi.org/10.1016/j.jafrearsci.2005.07.006>

- Azizi, M., Saibi, H., & Cooper, G. R. J. (2015). Mineral and structural mapping of the Aynak-Logar Valley (eastern Afghanistan) from hyperspectral remote sensing data and aeromagnetic data. *Arabian Journal of Geosciences*, 8, 10911-10918. <https://doi.org/10.1007/s12517-015-1993-2>
- Dada, S. S. (2008). Proterozoic evolution of the Nigeria–Boborema province. *Geological Society, London, Special Publications*, 294(1), 121-136. <https://doi.org/10.1144/SP294.7>
- Farhi, W., Boudella, A., Saibi, H., & Bounif, M. O. A. (2016). Integration of magnetic, gravity, and well data in imaging subsurface geology in the Ksar Hirane region (Laghouat, Algeria). *Journal of African Earth Sciences*, 124, 63-74. <https://doi.org/10.1016/j.jafrearsci.2016.09.013>
- Feng, X. T., Yu, Y., Feng, G. L., Xiao, Y. X., Chen, B. R., & Jiang, Q. (2016). Fractal behaviour of the microseismic energy associated with immediate rockbursts in deep, hard rock tunnels. *Tunnelling and Underground Space Technology*, 51, 98-107. <https://doi.org/10.1016/j.tust.2015.10.002>
- Hartman, R. R., Teskey, D. J., & Friedberg, J. L. (1971). A system for rapid digital aeromagnetic interpretation. *Geophysics*, 36(5), 891-918. <https://doi.org/10.1190/1.1440223>
- Hood, P. (1965). Gradient measurements in aeromagnetic surveying. *Geophysics*, 30(5), 891-902. <https://doi.org/10.1190/1.1439666>
- Kebede, H., Alemu, A., & Fisseha, S. (2020). Upward continuation and polynomial trend analysis as a gravity data decomposition, case study at Ziway-Shala basin, central Main Ethiopian rift. *Heliyon*, 6(1), e03292. <https://doi.org/10.1016/j.heliyon.2020.e03292>
- Kogbe, C. A., Ajakaiye, D. E., & Matheis, G. (1983). Confirmation of a rift structure along the Mid-Niger Valley, Nigeria. *Journal of African Earth Sciences (1983)*, 1(2), 127-131. [https://doi.org/10.1016/0899-5362\(83\)90004-0](https://doi.org/10.1016/0899-5362(83)90004-0)
- Ladipo, K. O. (1988). Paleogeography, sedimentation and tectonics of the Upper Cretaceous Anambra Basin, southeastern Nigeria. *Journal of African Earth Sciences (and the Middle East)*, 7(5-6), 865-871. [https://doi.org/10.1016/0899-5362\(88\)90029-2](https://doi.org/10.1016/0899-5362(88)90029-2)
- Li, Y., & Oldenburg, D. W. (1998). 3-D inversion of gravity data. *Geophysics*, 63(1), 109-119. <https://doi.org/10.1190/1.1444302>
- Likkason, O. K., & Ojo, S. B. (1999). Additional evidence from gravity for a basic intrusion in the Middle Niger Basin, Nigeria. *Journal of Mining & Geology*, 35(2), 171-181.
- Likkason, O. K., Singh, G. P., & Samaila, N. K. (2013). A Study of the middle benue trough (Nigeria) based on geological application and analyses of spectra of aeromagnetic data. *Energy Sources, Part A: Recovery, utilization, and environmental effects*, 35(8), 706-716. <https://doi.org/10.1080/15567036.2010.514588>
- MacLeod, I. N., Jones, K., & Dai, T. F. (1993). 3-D analytic signal in the interpretation of total magnetic field data at low magnetic latitudes. *Exploration geophysics*, 24(4), 679-688. <https://doi.org/10.1071/EG993679>
- Mammo, T. (2012). Analysis of gravity field to reconstruct the structure of Omo basin in SW Ethiopia and implications for hydrocarbon potential. *Marine and Petroleum Geology*, 29(1), 104-114. <https://doi.org/10.1016/j.marpetgeo.2011.08.013>
- Megwara, J. U., & Udensi, E. E. (2014). Structural analysis using aeromagnetic data: case study of parts of Southern Bida Basin, Nigeria and the surrounding basement rocks. *Earth science research*, 3(2), 27. <https://doi.org/10.5539/esr.v3n2p27>
- Menke, W. (2018). *Geophysical data analysis: Discrete inverse theory*. Academic press.
- Mohamed, H., Mizunaga, H., & Saibi, H. (2020). Computation of geophysical magnetic data for a buried 3-D hexahedral prism using the Gauss–Legendre quadrature method. *Near Surface Geophysics*, 18(5), 575-588. <https://doi.org/10.1002/nsg.12104>

- Murat, R. C. (1972). Stratigraphy and paleogeography of the Cretaceous and Lower Tertiary in Southern Nigeria. *African geology*, 1(1), 251-266.
- Nabighian, M. N. (1972). The analytic signal of two-dimensional magnetic bodies with polygonal cross-section: its properties and use for automated anomaly interpretation. *Geophysics*, 37(3), 507-517. <https://doi.org/10.1190/1.1440276>
- Nwachukwu, J. I. (1985). Petroleum prospects of Benue trough, Nigeria. *AAPG bulletin*, 69(4), 601-609. <https://doi.org/10.1306/AD46253D-16F7-11D7-8645000102C1865D>
- Nwajide, C. S. (2013). *Geology of Nigeria's sedimentary basins*. CSS Bookshop Limited.
- Obi, G. C. (2000). Depositional model for the Campanian-Maastrichtian Anambra Basin, Southern Nigeria. *Unpublished Ph. D. Thesis, University of Nigeria, Nsukka*, 291.
- Obi, G. C., Okogbue, C. O., & Nwajide, C. S. (2001). Evolution of the Enugu Cuesta: a tectonically driven erosional process. *Global Journal of Pure and Applied Sciences*, 7(2), 321-330. <https://doi.org/10.4314/gjpas.v7i2.16251>
- Ojo, O. J. (2012). Depositional environments and petrographic characteristics of Bida Formation around share-pategi, northern Bida basin, Nigeria. *Journal of Geography and Geology*, 4(1), 224. <https://doi.org/10.5539/jgg.v4n1p224>
- Ojo, O. J., & Akande, S. O. (2013). Petrographic facies, provenance and paleoenvironments of the Lokoja Formation southern Bida basin, Nigeria. *J. Min. Geol.*, 49(2), 93-109.
- Ojo, O. J., Bamidele, T. E., Adepoju, S. A., & Akande, S. O. (2020). Genesis and paleoenvironmental analysis of the ironstone facies of the Maastrichtian Patti Formation, Bida Basin, Nigeria. *Journal of African Earth Sciences*, 174, 104058. <https://doi.org/10.1016/j.jafrearsci.2020.104058>
- Phillips, J. D. (2000). Locating magnetic contacts: a comparison of the horizontal gradient, analytic signal, and local wavenumber methods. In *SEG Technical Program Expanded Abstracts 2000* (pp. 402-405). Society of Exploration Geophysicists. <https://doi.org/10.1190/1.1816078>
- Rahaman, M. A. O., Fadiya, S. L., Adekola, S. A., Coker, S. J., Bale, R. B., Olawoki, O. A., ... & Akande, W. G. (2019). A revised stratigraphy of the Bida Basin, Nigeria. *Journal of African Earth Sciences*, 151, 67-81. <https://doi.org/10.1016/j.jafrearsci.2018.11.016>
- Reyment, R. A. (1965). *Aspects of the geology of Nigeria: the stratigraphy of the Cretaceous and Cenozoic deposits* (Vol. 145). Ibadan: Ibadan university press.
- Roest, W. R., Verhoef, J., & Pilkington, M. (1992). Magnetic interpretation using the 3-D analytic signal. *Geophysics*, 57(1), 116-125. <https://doi.org/10.1190/1.1443174>
- Saibi, H., Aboud, E., & Gottsmann, J. (2015). Curie point depth from spectral analysis of aeromagnetic data for geothermal reconnaissance in Afghanistan. *Journal of African Earth Sciences*, 111, 92-99. <https://doi.org/10.1016/j.jafrearsci.2015.07.019>
- Salawu, N. B., Fatoba, J. O., Adebisi, L. S., Ajadi, J., Saleh, A., & Dada, S. S. (2020). Aeromagnetic and remote sensing evidence for structural framework of the middle Niger and Sokoto basins, Nigeria. *Physics of the Earth and Planetary Interiors*, 309, 106593. <https://doi.org/10.1016/j.pepi.2020.106593>
- Salem, A., Williams, S., Fairhead, J. D., Ravat, D., & Smith, R. (2007). Tilt-depth method: A simple depth estimation method using first-order magnetic derivatives. *The leading edge*, 26(12), 1502-1505. <https://doi.org/10.1190/1.2821934>
- Smith, R. S., Thurston, J. B., Dai, T. F., & MacLeod, I. N. (1998). iSPI™ - the improved source parameter imaging method. *Geophysical prospecting*, 46(2), 141-151. <https://doi.org/10.1046/j.1365-2478.1998.00084.x>
- Spector, A., & Grant, F. S. (1970). Statistical models for interpreting aeromagnetic data. *Geophysics*, 35(2), 293-302. <https://doi.org/10.1190/1.1440092>

- Talwani, M., Worzel, J. L., & Landisman, M. (1959). Rapid gravity computations for two-dimensional bodies with application to the Mendocino submarine fracture zone. *Journal of geophysical research*, 64(1), 49-59. <https://doi.org/10.1029/JZ064i001p00049>
- Telford, W. M., Geldart, L. P., & Sheriff, R. E. (1990). *Applied geophysics*. Cambridge university press.
- Thurston, J. B., & Smith, R. S. (1997). Automatic conversion of magnetic data to depth, dip, and susceptibility contrast using the SPI (TM) method. *Geophysics*, 62(3), 807-813. <https://doi.org/10.1190/1.1444190>
- Udensi, E. E., & Osazuwa, I. B. (2004). Spectral determination of depths to magnetic rocks under the Nupe Basin, Nigeria. *Nigerian Association of Petroleum Explorationists Bulletin*, 17, 22-27.
- Unomah, G. I. (1989). Petroleum evaluation of Upper Cretaceous Shales in Lower Benue Trough, Nigeria. *Unpublished Ph. D. Thesis, Univ. of Ibadan, Ibadan Nigeria*, 164.
- Werner, F. (1953). Interpretation of magnetic anomalies at sheet like bodies. *Geological Understanding Series, CC Arabok*, 43(6), 66-97.
- Zaher, M. A., Saibi, H., Mansour, K., Khalil, A., & Soliman, M. (2018). Geothermal exploration using airborne gravity and magnetic data at Siwa Oasis, Western Desert, Egypt. *Renewable and Sustainable Energy Reviews*, 82, 3824-3832. <https://doi.org/10.1016/j.rser.2017.10.088>



Copyright (c) 2023 by the authors. This work is licensed under a [Creative Commons Attribution-ShareAlike 4.0 International License](https://creativecommons.org/licenses/by-sa/4.0/).